

Development of coccolithophore-based transfer functions

B. Ausín et al.

Development of coccolithophore-based transfer functions in the Western Mediterranean Sea: a sea surface salinity reconstruction for the last 15.5 kyr

B. Ausín¹, I. Hernández-Almeida², J.-A. Flores¹, F.-J. Sierro¹, M. Grosjean², G. Francés³, and B. Alonso⁴

¹Department of Geology, University of Salamanca, Plaza de los Caídos s/n, 37008 Salamanca, Spain

²Institute of Geography and Oeschger Centre for Climate Change Research, University of Bern, Erlachstrasse 9a, 3012 Bern, 3012 Bern, Switzerland

³Department of Marine Geosciences, University of Vigo, Campus As Lagoas – Marcosende, 36310 Vigo, Spain

⁴Department of Marine Geosciences, Instituto de Ciencias del Mar (CSIC), Passeig Marítim de la Barceloneta, 37–49, 08003 Barcelona, Spain

Title Page

Abstract

Introduction

Conclusions

References

Tables

Figures



Back

Close

Full Screen / Esc

Printer-friendly Version

Interactive Discussion



Received: 4 August 2015 – Accepted: 5 August 2015 – Published: 21 August 2015

Correspondence to: B. Ausín (b_ausin@usal.es)

Published by Copernicus Publications on behalf of the European Geosciences Union.

CPD

11, 3759–3798, 2015

Development of coccolithophore-based transfer functions

B. Ausín et al.

[Title Page](#)

[Abstract](#)

[Introduction](#)

[Conclusions](#)

[References](#)

[Tables](#)

[Figures](#)



[Back](#)

[Close](#)

[Full Screen / Esc](#)

[Printer-friendly Version](#)

[Interactive Discussion](#)



Development of coccolithophore-based transfer functions

B. Ausín et al.

Title Page

Abstract

Introduction

Conclusions

References

Tables

Figures



Back

Close

Full Screen / Esc

Printer-friendly Version

Interactive Discussion



longitudinal gradients between the Atlantic Ocean and the Western Mediterranean in annual terms. In this confined basin, the estimation of changes in those environmental parameters is essential for determining Atlantic–Mediterranean water mass exchange through the Strait of Gibraltar in the past (Rohling and Bigg, 1998; Schmidt, 1998).

This exchange depends on variations in the hydrological cycle, ice-volume effects, and Mediterranean circulation patterns, which have a thermohaline origin (MEDOCGROUP, 1970).

The aim of this study is to explore the potential of coccolithophores for the development of quantitative reconstructions in the Western Mediterranean Sea. We study the response of coccolithophore assemblages from surface sediment samples from Atlantic Ocean and Mediterranean Sea to environmental variables. The resulting calibration model (transfer function) for salinity was used to reconstruct SSS changes at high-resolution in the Alboran Sea (Fig. 1a) for the last 25 kyr. The reliability of the reconstruction was assessed by analysis of the similarity between fossil and modern coccolithophore assemblages, and fossil ordination scores. Finally, centennial and millennial SSS changes are described and discussed, and compared to regional records of SST, organic matter preservation and continental aridity.

2 Materials and methods

2.1 Modern training set

2.1.1 Surface sediment samples

Initially, 117 core tops located around a horizontal transect along the Western Mediterranean Sea and near the Gulf of Cadiz in the Atlantic Ocean were selected. They had been retrieved at varying water depths ranging from 70 to 2620 m during several oceanographic surveys and were stored at the University of Vigo and at the Core Repository of the Institute of Marine Sciences – CSIC in Barcelona. The first cm (or the

2.3 Micropaleontological analyses

Both modern (surface sediment) and fossil (downcore) samples were prepared for coccolithophore analyses according to the techniques proposed by Flores and Sierro (1997). A polarized-light microscope at 1000× magnification was employed to identify and count at least 500 coccoliths in each sample, belonging to 21 different taxa. Species whose relative abundance was < 1 % in the first count were considered later in 20 visual fields in order to estimate their abundance accurately. The final relative abundance of each species in each sample was then recalculated. *Gephyrocapsa* specimens smaller than 3 μm were lumped together and designated “small *Gephyrocapsa*” (Flores et al., 1997). The “medium *Gephyrocapsa*” group was made up of *Gephyrocapsa* whose size was between 3 and 5 μm. The following species were split according to the size criteria: *E. huxleyi* (< 4 and > 4 μm) and *Gephyrocapsa oceanica* (< 5 and > 5 μm). Other taxa identified in this study were *Calcidiscus leptoporus*, *F. profunda*, *Gephyrocapsa caribbeanica*, *Gephyrocapsa muelleriae*, *Helicosphaera* spp., and *Syracosphaera* spp. (as dominant taxa). The rare taxa identified were *Braarudosphaera bigelowii*, *Calciosolenia murrayi*, *Coccolithus pelagicus* subsp. *braarudii*, *Coccolithus pelagicus* subsp. *pelagicus*, *Oolithotus fragilis*, *Pontosphaera* spp., *Rhabdosphaera clavigera*, *Umblicosphaera* spp. and *Umbellosphaera* spp.

Twenty-nine samples were finally eliminated from the initial modern data set owing to their high content (> 10 %) in obviously reworked nannofossils. These taxa belong to older stratigraphic levels (consistently older than the Pliocene in this study), meaning that they were resuspended and transported from their original location to the sample site, and lack any relationship with modern environmental conditions. Therefore, the final training set (Supplement) comprised 88 surface samples (Fig. 1b): 78 from the Western Mediterranean (58 from the Balearic Sea and 20 from the Alboran Sea) and 10 from the Atlantic Ocean.

CPD

11, 3759–3798, 2015

Development of coccolithophore-based transfer functions

B. Ausín et al.

Title Page

Abstract

Introduction

Conclusions

References

Tables

Figures



Back

Close

Full Screen / Esc

Printer-friendly Version

Interactive Discussion



colithophore training set explained uniquely by each significant environmental variable was calculated using variance partitioning.

Ordination analyses and variance partitioning were performed using the “vegan” package v.2.3. (Oksanen et al., 2015) for R (R Development Core Team, 2015).

2.4.2 Transfer function

Calibration models were calculated for the variable of interest (and every variable by means of exploratory analysis) using the weighted-averaging-partial least squares (WA-PLS) (ter Braak and Juggins, 1993; ter Braak et al., 1993) and the Modern Analog Technique (MAT) (Prell, 1985), both implemented in C2 version 1.4.3 software (Juggins, 2007). All models were calculated for the cross-validation predictions by bootstrapping (999 permutation cycles) (Birks, 1995). In MAT, the number of analogs resulting in the maximum coefficient of determination (R_{boot}^2) between the observed and predicted values and the lowest root-mean square error of prediction (RMSEP) (Telford et al., 2004) was calculated using an optimization set together with the usual training and test sets implemented in the “analoge” package for R (R Development Core Team, 2015). In WA-PLS, a decrease of 5% or more in RMSEP was required to retain the next component (Birks, 1995; ter Braak et al., 1993).

Telford et al. (2013) reported that SST reconstructions based on planktonic foraminifera census counts calibrated at a fixed depth and for a particular season might be biased. The most suitable calibration should be based on the depth and season that most influenced the coccolithophore fossil assemblage from core CEUTA10PC08. These were determined by testing the statistical significance of the summer, winter, and annual reconstructions of the variable of interest at 10 different depths of the upper photic zone from 10 to 300 m, following the procedure described by Telford et al. (2013), using the “paleoSig” package v.1.1-1 (Telford, 2015) for R (R Development Core Team, 2015).

Outliers may reduce the power of prediction of the calibration model as well as introducing undesirable effects in model coefficients (Birks, 1995). Potential outliers were

Development of coccolithophore-based transfer functions

B. Ausín et al.

Title Page

Abstract

Introduction

Conclusions

References

Tables

Figures



Back

Close

Full Screen / Esc

Printer-friendly Version

Interactive Discussion



determined as those whose absolute residual was higher than the mean SD of the observed values (Edwards et al., 2004).

A combination of the highest R_{boot}^2 and the lowest RMSEP was used as a criterion for the quality prediction of the model. The graphical representations of the observed values against the values predicted by the model and the residuals against the predicted values were used as a diagnosis of the model.

2.4.3 Derived reconstruction and evaluation

MAT and WA-PLS were applied to the fossil coccolithophore assemblages of core CEUTA10PC08, which were previously square-root transformed. In order to assess the quality of the modern analogs for the fossil (downcore) samples, the squared chord distance between each fossil sample and each sample in the modern training set (Overpeck et al., 1985) was calculated with MAT using C2 version 1.4.3 software (Juggins, 2007). A squared chord distance below the 10th percentile would be considered good, while values above this cutoff would represent assemblages with poor analogs (Simpson, 2007).

The first axis of the PCA analyses of the fossil dataset ($PC1_{fossil}$) shows the most important changes in the composition of the fossil coccolithophore assemblage. Comparison between $PC1_{fossil}$ and the reconstructed variable of interest was used to assess whether the reconstruction could be considered representative of the major ecological changes of the fossil assemblage (Juggins, 2013).

3 Results

3.1 Geographical distribution of coccolithophores

The geographical distribution of the main coccolithophore taxa is shown in Fig. 2. The relative abundance of *E. huxleyi* $< 4 \mu\text{m}$ increases from the southern Spanish coast to the northern African coast, and high values are observed around the mouth of the Ebro

Development of coccolithophore-based transfer functions

B. Ausín et al.

Title Page

Abstract

Introduction

Conclusions

References

Tables

Figures



Back

Close

Full Screen / Esc

Printer-friendly Version

Interactive Discussion



values from both models approach the diagonal of slope one (that indicates perfect predictions) reasonably well (Fig. 4d and e). The residuals for MAT and WA-PLS2 models (Fig. 4f and g) are equally distributed around zero and show no apparent trends.

3.4 SSS reconstruction

The SSS reconstructions for core CEUTA10PC08 derived from both MAT and WA-PLS2 are very similar (Fig. 5a and b), with same range of SSS values. These only differ during the stadials associated with Heinrich Events 2 and 1 (H2 and H1), when the WA-PLS2-estimated SSS shows more pronounced salinity decreases.

The SSS reconstructions obtained from core CEUTA10PC08 (Fig. 5a) can be divided into three intervals: (i) the period from 25.5 to 15.5 ka is characterized by higher values, ranging between 37.8 and 37 psu. Lower values are found from 20 to 18 ka followed by a drop of 0.8 psu at 17.3 ka, (ii) the period from 15.5 to 9 ka shows fast changes and large oscillations. An abrupt decrease from 37.9 to 36.9 psu is recognized at 15 ka, followed by large peaks of high values at 12.8, 11.1, and 10.2 ka; and (iii) the period from 9 to 4.5 ka records the lowest values, ranging between 37 and 36.5 psu and shows a general decreasing trend.

The errors associated with both SSS reconstruction are of a similar magnitude for the last 25 kyr (Fig. 5a). Squared chord distances between fossil and modern assemblages (Fig. 5b) revealed that many samples from 25.5 to 16 ka were above the 10th percentile. The comparison between $PC1_{\text{fossil}}$ and the SSS reconstruction is shown in Fig. 5c, showing general good agreement, especially for the last 16 kyr.

4 Discussion

4.1 Geographic coccolithophore distribution and SSS

E. huxleyi (< 4 μm) and *small Gephyrocapsa* (< 3 μm) are very abundant (83% on average) and widespread in the Western Mediterranean (Fig. 2a and b) as previ-

Development of coccolithophore-based transfer functions

B. Ausín et al.

[Title Page](#)[Abstract](#)[Introduction](#)[Conclusions](#)[References](#)[Tables](#)[Figures](#)[Back](#)[Close](#)[Full Screen / Esc](#)[Printer-friendly Version](#)[Interactive Discussion](#)

Development of coccolithophore-based transfer functions

B. Ausín et al.

Title Page

Abstract

Introduction

Conclusions

References

Tables

Figures



Back

Close

Full Screen / Esc

Printer-friendly Version

Interactive Discussion



et al., 1998; Paasche et al., 1996; Schouten et al., 2006), in both culture experiments and marine surface sediment samples. Nevertheless, findings by Oviedo et al. (2015) point toward the same direction of variability of coccolithophore assemblages in the Mediterranean Sea controlled by salinity and/or related variables. It is worth to mention that salinity influences solubility of CO_3^{2-} through several paths: the solubility of free carbon dioxide in water, the solubility product constants, the concentration of the ion hydrogen, and the quantity of calcium in the water (Trask, 1936). Based on this strong relationship, salinity could be influencing coccolithophore distribution through coccolith calcification processes. In contrast, Bollmann and Herrle (2009) have proposed an alternative hypothesis, suggesting that salinity influences coccolithophores through cell turgor regulation linked to osmotic processes.

Although there is no clear consensus about the mechanism through which salinity influence coccolithophore associations, many other studies point to a strong link between this variable and coccolithophore species. In the Japan Sea, salinity has been proposed to have an ecological or physiological influence on the production of alkenone and alkenoates, which are organic compounds mainly produced by *Emiliania* and *Gephyrocapsa* genus (Fujine et al., 2006). In the Baltic Sea, alkenone unsaturation ratios have been found to be significantly correlated with salinity (Blanz et al., 2005). In the Mediterranean Sea, Knappertsbusch (1993) studied the distribution of extant coccolithophore species in relation to in situ temperature and salinity data. A good correspondence was only found between coccolithophore species and the environmental parameters under study, indicating that *G. oceanica* was linearly correlated with salinity. Moreover, salinity has proven to be important to other marine unicellular planktonic groups such as diatoms (Fritz et al., 1991; Jiang et al., 2014; Li et al., 2012) and dinoflagellate cysts (Jansson et al., 2014, and references therein), reinforcing the hypothesis of salinity as an important variable for planktonic communities in semi-enclosed basins.

4.2 Transfer function quality

A general good fit can be deduced for both models, although MAT was seen to perform slightly better from a higher R_{boot}^2 and a lower RMSEP (Table 2) and plotted predicted values compared with observed values (Fig. 4). The intermediate values of the salinity gradient are less well represented than the more extreme values (Fig. 4d and e). Unevenness can bias the RMSEP leading to overestimation of the predictive power of the model (Telford and Birks, 2011). While an even distribution would be always desirable, unevenness is a feature inherent to most training sets from oceanic environments. In this case, it is not severe and the observations, although unevenly distributed along the salinity gradient, do not leave gaps. The distribution of the residuals (Fig. 4f and g) indicates the adequacy of the model.

4.3 Downcore SSS reconstruction

The derived MAT and WA-PLS2 SSS reconstructions (Fig. 5a) are very similar. Nevertheless, WA-PLS2 shows more marked salinity decreases than MAT during the H2 (25.2–23.7 ka) and H1 (17.4–15.9 ka). Unlike WA-PLS, MAT does not consider the entire dataset when calculating the species optima, only the most taxonomically similar analogs, being more sensitive to local conditions (Telford and Birks, 2009). Fossil samples lack good analogs for the H2 and H1, coinciding with large peaks of *E. huxleyi* ($> 4 \mu\text{m}$) (Fig. 5b). H2 and H1 have been linked to the entry of fresher water originating from the North Atlantic ice melting in the Western Mediterranean Sea (Cacho et al., 1999; Melki, 2011; Sierro et al., 2005), suggesting a link between the high abundances of *E. huxleyi* ($> 4 \mu\text{m}$) and lower salinities in the past. By contrast, Bollmann and Herle (2007) reported a significant current correlation between *E. huxleyi* ($> 4 \mu\text{m}$) and higher salinities from the study of globally distributed core-top samples. These authors used this relationship to estimate salinity values during the LGM. Interestingly, they observed several overestimations with regard to other published values in samples characterized by high relative abundances of *E. huxleyi* ($> 4 \mu\text{m}$). These discrepancies

suggest that high percentages/presence of *E. huxleyi* ($> 4 \mu\text{m}$) in the fossil record lacks modern analogs, as indicated by the high dissimilarity between fossil samples with high percentages of this species and modern samples (Fig. 5b).

Owing to MAT is strongly dependent upon on the analogs selected (Telford and Birks, 2009) and WA-PLS2 reconstruction for H2 and H1 is more coherent with a freshwater inflow scenario, it seems WA-PLS2 affords more reliable values than MAT. Consequently, WA-PLS2-estimated SSS is chosen for final interpretations.

Transfer functions assume that the ecological response of organisms to either the environmental variable of interest or to the linear combination of this important variable with others has not changed significantly over the time span represented by the fossil assemblage (Birks, 1995). The good agreement observed between $\text{PC1}_{\text{fossil}}$ and reconstructed SSS patterns from 16 ka onwards (Fig. 5c) suggests that the SSS transfer function fulfills this assumption back to 16 ka. Larger differences are observed from 25 to 16 ka, possibly promoted by the situation of the absence of analogs during this period discussed above.

4.4 SSS changes in the Alboran Sea over the last 15.5 kyr

The SSS reconstruction (Fig. 6a) might involve additional uncertainty during part of the LGM (from 25 to 18 ka), H2 and H1 derived from the lack of analogs. Consequently, the SSS reconstruction for that time span will not be discussed here.

4.4.1 Oldest Dryas

An abrupt decrease in salinity of 0.8 psu occurred at 15.5 ka. This change is not supported by the findings of Fletcher and Sánchez Goñi (2008) or those of Combourieu Nebout et al. (2009) who, using pollen records from two sites in the Western Mediterranean, identified arid conditions in the southern Iberian Peninsula. The global sea-level rise of ~ 20 m during meltwater pulse 1A (mwp-1A) has been dated at 14.6 ka (Bard et al., 1996; Weaver et al., 2003), simultaneous to the onset of the Bølling–

Development of coccolithophore-based transfer functions

B. Ausín et al.

Title Page

Abstract

Introduction

Conclusions

References

Tables

Figures



Back

Close

Full Screen / Esc

Printer-friendly Version

Interactive Discussion



Allerød. Since this section covers 3000 yr with no control point (Fig. 6a), it could be an artifact of poorly constrained chronology for this time interval. Nevertheless, this seems unlikely since other authors (Duplessy et al., 1992; Emeis et al., 2000; Kallel et al., 1997) have reported similar abrupt SSS decreases in different regions of the Mediterranean Sea and the Atlantic Ocean at this time.

In particular, Duplessy et al. (1992) observed a SSS decrease of about 2.5 psu in the Atlantic Ocean west of the Strait of Gibraltar during the Oldest Dryas in northwestern Europe and related it to the meltwater release from the Barents and the Fennoscandian ice sheets. These authors also argued that such minor injections of freshwater would have been insufficient to trigger the observed drop in salinity, and proposed an additional feedback from changes in the hydrological cycle and water advection to promote changes in the thermohaline circulation and the observed changes in SSS.

4.4.2 Bølling–Allerød (B–A)

The SSS values are generally low for the B–A, the Bølling being fresher than the Allerød, both separated by the Older-Dryas (GI-1d) interval (Fig. 6a). Owing to the global sea-level rise during the B–A, and specifically during the mwp-1A between 13.5 and 14.1 ka, a greater volume of AW would have entered through the Strait, decreasing the average SSS. In addition, wetter conditions would have contributed to this freshening. Enhanced rainfall and increased river discharge have already been inferred from diatom assemblages, sediment grain-size, pollen records, elemental ratios and coccolithophore records in the Western Mediterranean during the B–A (Ausín et al., 2015; Bárcena et al., 2001; Combourieu Nebout et al., 2009; Frigola et al., 2008; Martínez-Ruiz et al., 2015; Rodrigo-Gámiz et al., 2011). This period of reduced salinity also coincides with the highest values of total concentration of C_{37} alkenones, a proxy of organic matter preservation (Cacho et al., 2002), from a nearby core located off the coast of Malaga (Ausín et al., 2015) (Fig. 6a and b), linked to the development of the Organic-Rich Layer (ORL-1) (Cacho et al., 2002). The ORL-1 appears in many sediment cores from the Alboran Sea as a consequence of the accumulation of high amounts of or-

Development of coccolithophore-based transfer functions

B. Ausín et al.

Title Page

Abstract

Introduction

Conclusions

References

Tables

Figures



Back

Close

Full Screen / Esc

Printer-friendly Version

Interactive Discussion



Alboran Sea and the onset of the decline of the African Humid Period. SSS remained low from 7.4 to 4.5 ka, close to its present values.

A broader understanding of the ecological link between coccolithophore species and environmental parameters would be desirable in order to be able to place coccolithophore-based transfer functions within the ecological context in future works. Nevertheless, the diverse statistical tests performed in this study and the strong emphasis placed on assessing the validity and reliability of both the model and the reconstruction do reveal the potential of coccolithophores for developing transfer functions. The derived transfer function provides a potential independent proxy for quantitative reconstructions of SSS changes in other locations of the Western Mediterranean Sea over the last 15.5 kyr.

The Supplement related to this article is available online at doi:10.5194/cpd-11-3759-2015-supplement.

Acknowledgements. B. Ausín is sincerely grateful to the Core Repository of the Institute of Marine Sciences- CSIC at Barcelona and the University of Vigo for the core-top samples supply. This study was supported by the FPU grant AP2010-2559 of the Ministry of Education of Spain given to B. Ausín and by the Consolider Ingenio “GRACCIE” program CSD 2007-00067, the program SA263U14 of Junta de Castilla y León, and the programs: CGL2011-26493, VACLIDP339, CTM2008-06399-C04/MAR, CTM 2012-39599-C03-02/03 and MOWER (CTM 2012-39599-CO3-02/03) of the Spanish Ministry of Economy and Competitiveness.

References

- Álvarez, M. C., Amore, F. O., Cros, L., Alonso, B., and Alcántara-Carrió, J.: Coccolithophore biogeography in the Mediterranean Iberian margin, *Revista Española de Micropaleontología*, 42, 359–372, 2010.
- Alley, R. B., Mayewski, P. A., Sowers, T., Stuiver, M., Taylor, K. C., and Clark, P. U.: Holocene climatic instability: a prominent, widespread event 8200 yr ago, *Geology*, 25, 483–486, 1997.

Development of coccolithophore-based transfer functions

B. Ausín et al.

Title Page

Abstract

Introduction

Conclusions

References

Tables

Figures



Back

Close

Full Screen / Esc

Printer-friendly Version

Interactive Discussion



Development of coccolithophore-based transfer functions

B. Ausín et al.

Title Page

Abstract

Introduction

Conclusions

References

Tables

Figures



Back

Close

Full Screen / Esc

Printer-friendly Version

Interactive Discussion



- Ausín, B., Flores, J. A., BÁCena, M. A., Sierro, F. J., Francés, G., Gutiérrez-Arnillas, E., Hernández-Almeida, I., Martrat, B., Grimalt, J. O., and Cacho, I.: Coccolithophore productivity and surface water dynamics in the Alboran Sea during the last 25 kyr, *Palaeogeogr. Palaeoclimatol.*, 418, 126–140, 2015.
- 5 BÁCena, M. A., Cacho, I., Abrantes, F., Sierro, F. J., Grimalt, J. O., and Flores, J. A.: Paleoproductivity variations related to climatic conditions in the Alboran Sea (western Mediterranean) during the last glacial–interglacial transition: the diatom record, *Palaeogeogr. Palaeoclimatol.*, 167, 337–357, 2001.
- 10 Bard, E., Hamelin, B., Arnold, M., Montaggioni, L., Cabioch, G., Faure, G., and Rougerie, F.: Deglacial sea-level record from Tahiti corals and the timing of global meltwater discharge, *Nature*, 382, 241–244, 1996.
- Baumann, K. H., Andruleit, H., Boeckel, B., Geisen, M., and Kinkel, H.: The significance of extant coccolithophores as indicators of ocean water masses, surface water temperature, and palaeoproductivity: a review, *Palaeont. Z.*, 79, 93–112, 2005.
- 15 Beaufort, L., Lancelot, Y., Camberlin, P., Cayre, O., Vincent, E., Bassinot, F., and Labeyrie, L.: Insolation cycles as a major control of equatorial Indian Ocean primary production, *Science*, 278, 1451–1454, 1997.
- Beaufort, L., de Garidel-Thoron, T., Mix, A. C., and Pisias, N. G.: ENSO-like forcing on oceanic primary production during the Late Pleistocene, *Science*, 293, 2440–2444, 2001.
- 20 Beaufort, L., Probert, I., de Garidel-Thoron, T., Bendif, E. M., Ruiz-Pino, D., Metzli, N., Goyet, C., Buchet, N., Coupel, P., Grelaud, M., Rost, B., Rickaby, R. E. M., and de Vargas, C.: Sensitivity of coccolithophores to carbonate chemistry and ocean acidification, *Nature*, 476, 80–83, 2011.
- Bèthoux, J. P.: Budgets of the Mediterranean Sea. Their dependence on the local climate and on the characteristics of the Atlantic waters, *Oceanol. Acta*, 2, 157–163, 1979.
- 25 Birks, H. J. B.: Quantitative palaeoenvironmental reconstructions, in: *Statistical Modelling of Quaternary Science Data*, technical guide 5, edited by: Maddy, D. and Brew, J. S., Quaternary Research Association, Cambridge, 271 pp., 1995.
- Blanz, T., Emeis, K.-C., and Siegel, H.: Controls on alkenone unsaturation ratios along the salinity gradient between the open ocean and the Baltic Sea, *Geochim. Cosmochim. Ac.*, 69, 3589–3600, 2005.
- 30 Bollmann, J. and Herrle, J. O.: Morphological variation of *Emiliania huxleyi* and sea surface salinity, *Earth Planet. Sc. Lett.*, 255, 273–288, 2007.

Development of coccolithophore-based transfer functions

B. Ausín et al.

[Title Page](#)

[Abstract](#)

[Introduction](#)

[Conclusions](#)

[References](#)

[Tables](#)

[Figures](#)



[Back](#)

[Close](#)

[Full Screen / Esc](#)

[Printer-friendly Version](#)

[Interactive Discussion](#)



Bollmann, J., Herrle, J. O., Cortés, M. Y., and Fielding, S. R.: The effect of sea water salinity on the morphology of *Emiliania huxleyi* in plankton and sediment samples, *Earth Planet. Sc. Lett.*, 284, 320–328, 2009.

Boyer, T. P., Antonov, J. I., Baranova, O. K., Coleman, C., Garcia, H. E., Grodsky, A., Johnson, D. R., Locarnini, R. A., Mishonov, A. V., O'Brien, T. D., Paver, C. R., Reagan, J. R., Seidov, D., Smolyar, I. V., and Zweng, M. M.: World ocean database 2013, in: NOAA Atlas NESDIS 72, edited by: Levitus, S. and Mishonov, A., Silver Spring, MD, 209, 2013.

Cacho, I., Grimalt, J. O., Pelejero, C., Canals, M., Sierro, F. J., Flores, J. A., and Shackleton, N.: Dansgaard–Oeschger and Heinrich Event imprints in Alboran Sea paleotemperatures, *Paleoceanography*, 14, 698–705, 1999.

Cacho, I., Grimalt, J. O., Canals, M., Sbaiffi, L., Shackleton, N. J., Schönfeld, J., and Zahn, R.: Variability of the western Mediterranean Sea surface temperature during the last 25 000 years and its connection with the Northern Hemisphere climatic changes, *Paleoceanography*, 16, 40–52, 2001.

Cacho, I., Grimalt, J. O., and Canals, M.: Response of the Western Mediterranean Sea to rapid climatic variability during the last 50 000 years: a molecular biomarker approach, *J. Marine Syst.*, 33–34, 253–272, 2002.

Combourieu Nebout, N., Peyron, O., Dormoy, I., Desprat, S., Beaudouin, C., Kotthoff, U., and Marret, F.: Rapid climatic variability in the west Mediterranean during the last 25 000 years from high resolution pollen data, *Clim. Past*, 5, 503–521, doi:10.5194/cp-5-503-2009, 2009.

Cros, L. and Fortuño, J.-M.: Atlas of northwestern Mediterranean coccolithophores, *Sci. Mar.*, 66, 7–182, 2002.

deMenocal, P., Ortiz, J., Guilderson, T., Adkins, J., Sarnthein, M., Baker, L., and Yarusinsky, M.: Abrupt onset and termination of the African Humid Period: rapid climate responses to gradual insolation forcing, *Quaternary Sci. Rev.*, 19, 347–361, 2000.

Dormoy, I., Peyron, O., Combourieu Nebout, N., Goring, S., Kotthoff, U., Magny, M., and Pross, J.: Terrestrial climate variability and seasonality changes in the Mediterranean region between 15 000 and 4000 years BP deduced from marine pollen records, *Clim. Past*, 5, 615–632, doi:10.5194/cp-5-615-2009, 2009.

Duplessy, J. C., Labeyrie, L., Arnold, M., Paterne, M., Duprat, J., and van Weering, T. C. E.: Changes in surface salinity of the North Atlantic Ocean during the last deglaciation, *Nature*, 358, 485–488, 1992.

Development of coccolithophore-based transfer functions

B. Ausín et al.

Title Page

Abstract

Introduction

Conclusions

References

Tables

Figures

◀

▶

◀

▶

Back

Close

Full Screen / Esc

Printer-friendly Version

Interactive Discussion



Edwards, R. J., van de Plassche, O., Gehrels, W. R., and Wright, A. J.: Assessing sea-level data from Connecticut, USA, using a foraminiferal transfer function for tide level, *Mar. Micropaleontol.*, 51, 239–255, 2004.

5 Emeis, K.-C., Struck, U., Schulz, H.-M., Rosenberg, R., Bernasconi, S., Erlenkeuser, H., Sakamoto, T., and Martinez-Ruiz, F.: Temperature and salinity variations of Mediterranean Sea surface waters over the last 16 000 years from records of planktonic stable oxygen isotopes and alkenone unsaturation ratios, *Palaeogeogr. Palaeoclimatol.*, 158, 259–280, 2000.

Fairbanks, R. G.: A 17 000 year glacio-eustatic sea level record; influence of glacial melting rates on the Younger Dryas event and deep-ocean circulation, *Nature*, 342, 637–642, 1989.

10 Fielding, S. R., Herrle, J. O., Bollmann, J., Worden, R. H., and Montagned, D. J. S.: Assessing the applicability of *Emiliania huxleyi* coccolith morphology as a sea-surface salinity proxy, *Limnol. Oceanogr.*, 54, 1475–1480, 2009.

Fletcher, W. J. and Sánchez Goñi, M. F.: Orbital- and sub-orbital-scale climate impacts on vegetation of the western Mediterranean basin over the last 48 000 yr, *Quaternary Res.*, 70, 451–464, 2008.

15 Fletcher, W. J., Sanchez Goñi, M. F., Peyron, O., and Dormoy, I.: Abrupt climate changes of the last deglaciation detected in a Western Mediterranean forest record, *Clim. Past*, 6, 245–264, doi:10.5194/cp-6-245-2010, 2010.

Flores, J. A. and Sierro, F. J.: Revised technique for calculation of calcareous nannofossil accumulation rates, *Micropaleontology*, 43, 321–324, 1997.

20 Flores, J. A., Sierro, F. J., Francés, G., Vázquez, A., and Zamarréño, I.: The last 100 000 years in the western Mediterranean: sea surface water and frontal dynamics as revealed by coccolithophores, *Mar. Micropaleontol.*, 29, 351–366, 1997.

Frigola, J., Moreno, A., Cacho, I., Canals, M., Sierro, F. J., Flores, J. A., and Grimalt, J. O.: Evidence of abrupt changes in Western Mediterranean deep water circulation during the last 50 kyr: a high-resolution marine record from the Balearic Sea, *Quatern. Int.*, 181, 88–104, 2008.

Fritz, S. C., Juggins, S., Battarbee, R. W., and Engstrom, D. R.: Reconstruction of past changes in salinity and climate using a diatom-based transfer function, *Nature*, 352, 706–708, 1991.

30 Fujine, K., Yamamoto, M., Tada, R., and Kido, Y.: A salinity-related occurrence of a novel alkenone and alkenoate in Late Pleistocene sediments from the Japan Sea, *Org. Geochem.*, 37, 1074–1084, 2006.

Development of coccolithophore-based transfer functions

B. Ausín et al.

Title Page

Abstract

Introduction

Conclusions

References

Tables

Figures



Back

Close

Full Screen / Esc

Printer-friendly Version

Interactive Discussion



García, H. E., Locarnini, R. A., Boyer, T. P., Antonov, J. I., Baranova, O. K., Zweng, M. M., Reagan, J. R., and Johnson, D. R.: World ocean atlas 2013, volume 3: dissolved oxygen, apparent oxygen utilization, and oxygen saturation, in: NOAA Atlas NESDIS 75, edited by: Levitus, S. and Mishonov, A., 27 pp., 2014a.

García, H. E., Locarnini, R. A., Boyer, T. P., Antonov, J. I., Baranova, O. K., Zweng, M. M., Reagan, J. R., and Johnson, D. R.: World ocean atlas 2013, volume 4: dissolved inorganic nutrients (phosphate, nitrate, silicate), in: NOAA Atlas NESDIS 76, edited by: Levitus, S. and Mishonov, A., 25 pp., 2014b.

Giraudeau, J. and Rogers, J.: Phytoplankton biomass and sea-surface temperature estimates from sea-bed distribution of nannofossils and planktonic foraminifera in the Benguela upwelling system, *Micropaleontology*, 40, 275–285, 1994.

Goyet, C., Healy, R. J., and Ryan, P. D.: Global Distribution of Total Inorganic Carbon and Total Alkalinity Below the Deepest Winter Mixed Layer Depths, ORNL/CDIAC-127, NDP-076, Carbon Dioxide Information Analysis Center, Oak Ridge National Laboratory, US Department of Energy, Oak Ridge, TN, 2000.

Green, J. C., Heimdal, B. R., Paasche, E., and Moate, R.: Changes in calcification and the dimensions of coccoliths of *Emiliana huxleyi* (Haptophyta) grown at reduced salinities, *Phycologia*, 37, 121–131, 1998.

Guerreiro, C., Oliveira, A., de Stigter, H., Cachão, M., Sá C, Borges, C., Cros, L., Santos, A., Fortuño, J.-M., and Rodrigues, A.: Late winter coccolithophore bloom off central Portugal in response to river discharge and upwelling, *Cont. Shelf. Res.*, 59, 65–83, 2013.

Guerreiro, C., Sá C, de Stigter, H., Oliveira, A., Cachão, M., Cros, L., Borges, C., Quaresma, L., Santos, A. I., Fortuño, J.-M., and Rodrigues, A.: Influence of the Nazaré Canyon, central Portuguese margin, on late winter coccolithophore assemblages, *Deep-Sea Res. Pt. II*, 104, 335–358, 2014.

Incarbona, A., Martrat, B., Di Stefano, E., Grimalt, J. O., Pelosi, N., Patti, B., and Tranchida, G.: Primary productivity variability on the Atlantic Iberian Margin over the last 70 000 years: evidence from coccolithophores and fossil organic compounds, *Paleoceanography*, 25, PA2218, doi:10.1029/2008PA001709, 2010.

Jansson, I.-M., Mertens, K. N., Head, M. J., de Vernal, A., Londeix, L., Marret, F., Matthiessen, J., and Sangiorgi, F.: Statistically assessing the correlation between salinity and morphology in cysts produced by the dinoflagellate *Protoceratium reticulatum* from sur-

Development of coccolithophore-based transfer functions

B. Ausín et al.

Title Page

Abstract

Introduction

Conclusions

References

Tables

Figures



Back

Close

Full Screen / Esc

Printer-friendly Version

Interactive Discussion



- Millot, C.: Circulation in the Western Mediterranean Sea, *J. Marine Syst.*, 20, 423–442, 1999.
- Monterey, G. and Levitus, S.: Seasonal Variability of Mixed Layer Depth for the World Ocean, NOAA Atlas NESDIS 14, US Gov. Printing Office, Wash., DC, 96 pp., 1997.
- Oksanen, J., Blanchet, F. G., Kindt, R., Legendre, P., Minchin, P. R., O'Hara, B., Simpson, G. L., Solymos, P., Stevens, M. H. H., and Wagner, H.: *Vegan: Community Ecology Package*, R package version 2.3-0., 2015.
- Overpeck, J. T., Webb, T., and Prentice, I. C.: Quantitative interpretation of fossil pollen spectra: dissimilarity coefficients and the method of modern analogs, *Quaternary Res.*, 23, 87–108, 1985.
- Oviedo, A., Ziveri, P., Álvarez, M., and Tanhua, T.: Is coccolithophore distribution in the Mediterranean Sea related to seawater carbonate chemistry?, *Ocean Sci.*, 11, 13–32, doi:10.5194/os-11-13-2015, 2015.
- Paasche, E., Brubak, S., Skattebøl, S., Young, J. R., and Green, J. C.: Growth and calcification in the coccolithophorid *Emiliania huxleyi* (Haptophyceae) at low salinities, *Phycologia*, 35, 394–403, 1996.
- Prell, W. L.: *The Stability of Low-Latitude Sea-Surface Temperatures: an Evaluation of the CLIMAP Reconstruction with Emphasis on the Positive SST Anomalies*, Department of Energy, Washington, DC, 1985.
- R Core Team: *R: A language and environment for statistical computing*, R Foundation for Statistical Computing, Vienna, Austria, available at: <http://www.R-project.org> (last access: 28 July 2015), 2015.
- Renssen, H., Brovkin, V., Fichefet, T., and Goosse, H.: Holocene climate instability during the termination of the African Humid Period, *Geophys. Res. Lett.*, 30, 1184, doi:10.1029/2002GL016636, 2003.
- Ritchie, J. C., Eyles, C. H., and Haynes, C. V.: Sediment and pollen evidence for an early to mid-Holocene humid period in the eastern Sahara, *Nature*, 330, 645–647, 1985.
- Rodrigo-Gámiz, M., Martínez-Ruiz, F., Jiménez-Espejo, F. J., Gallego-Torres, D., Nieto-Moreno, V., Romero, O., and Ariztegui, D.: Impact of climate variability in the western Mediterranean during the last 20 000 years: oceanic and atmospheric responses, *Quaternary Sci. Rev.*, 30, 2018–2034, 2011.
- Rogerson, M., Cacho, I., Jimenez-Espejo, F., Reguera, M. I., Sierro, F. J., Martinez-Ruiz, F., Frigola, J., and Canals, M.: A dynamic explanation for the origin of the western Mediterranean

Development of coccolithophore-based transfer functions

B. Ausín et al.

Title Page

Abstract

Introduction

Conclusions

References

Tables

Figures



Back

Close

Full Screen / Esc

Printer-friendly Version

Interactive Discussion



organic-rich layers, *Geochem. Geophys. Geosy.*, 9, Q07U01, doi:10.1029/2007GC001936, 2008.

Rohling, E. J. and Bigg, G. R.: Paleosalinity and $\delta^{18}\text{O}$: A critical assessment, *J. Geophys. Res.-Oceans*, 103, 1307–1318, 1998.

Saavedra-Pellitero, M., Flores, J. A., Lamy, F., Sierro, F. J., and Cortina, A.: Coccolithophore estimates of paleotemperature and paleoproductivity changes in the southeast Pacific over the past 27 kyr, *Paleoceanography*, 26, PA1201, doi:10.1029/2009PA001824, 2011.

Saavedra-Pellitero, M., Baumann, K. H., Hernández-Almeida, I., Flores, J. A., and Sierro, F. J.: Modern sea surface productivity and temperature estimations off Chile as detected by coccolith accumulation rates, *Palaeogeogr. Palaeoclimatol.*, 392, 534–545, 2013.

Sbaffi, L., Wezel, F. C., Curzi, G., and Zoppi, U.: Millennial- to centennial-scale palaeoclimatic variations during Termination I, and the Holocene in the central Mediterranean Sea, *Global Planet. Change*, 40, 201–217, 2004.

Schlitzer, R.: Ocean Data View, available at: <http://odv.awi.de> (last access: 22 July 2015), 2014.

Schmidt, G. A.: Oxygen-18 variations in a global ocean model, *Geophys. Res. Lett.*, 25, 1201–1204, 1998.

Schouten, S., Ossebaar, J., Schreiber, K., Kienhuis, M. V. M., Langer, G., Benthien, A., and Bijma, J.: The effect of temperature, salinity and growth rate on the stable hydrogen isotopic composition of long chain alkenones produced by *Emiliania huxleyi* and *Gephyrocapsa oceanica*, *Biogeosciences*, 3, 113–119, doi:10.5194/bg-3-113-2006, 2006.

Sierro, F. J., Hodell, D. A., Curtis, J. H., Flores, J. A., Reguera, I., Colmenero-Hidalgo, E., Bárcena, M. A., Grimalt, J. O., Cacho, I., Frigola, J., and Canals, M.: Impact of iceberg melting on Mediterranean thermohaline circulation during Heinrich events, *Paleoceanography*, 20, PA2019, doi:10.1029/2004PA001051, 2005.

Simpson, G. L.: Analogue methods in palaeoecology: using the analogue package, *J. Stat. Softw.*, 22, 1–19, 2007.

Telford, R. J.: PalaeoSig: Significance Tests of Quantitative Palaeoenvironmental Reconstructions, R package version 1.1-3, 2015.

Telford, R. J. and Birks, H. J. B.: Evaluation of transfer functions in spatially structured environments, *Quaternary Sci. Rev.*, 28, 1309–1316, 2009.

Telford, R. J. and Birks, H. J. B.: A novel method for assessing the statistical significance of quantitative reconstructions inferred from biotic assemblages, *Quaternary Sci. Rev.*, 30, 1272–1278, 2011.

Zweng, M. M., Reagan, J. R., Antonov, J. I., Locarnini, R. A., Mishonov, A. V., Boyer, T. P., Garcia, H. E., Baranova, O. K., Johnson, D. R., Seidov, D., and Biddle, M. M.: World ocean atlas 2013, volume 2: salinity, in: NOAA Atlas NESDIS 74, edited by: Levitus, S. and Mishonov, A., 39 pp., 2013.

CPD

11, 3759–3798, 2015

Development of coccolithophore-based transfer functions

B. Ausín et al.

[Title Page](#)

[Abstract](#)

[Introduction](#)

[Conclusions](#)

[References](#)

[Tables](#)

[Figures](#)



[Back](#)

[Close](#)

[Full Screen / Esc](#)

[Printer-friendly Version](#)

[Interactive Discussion](#)



Development of coccolithophore-based transfer functions

B. Ausín et al.

[Title Page](#)

[Abstract](#)

[Introduction](#)

[Conclusions](#)

[References](#)

[Tables](#)

[Figures](#)

[◀](#)

[▶](#)

[◀](#)

[▶](#)

[Back](#)

[Close](#)

[Full Screen / Esc](#)

[Printer-friendly Version](#)

[Interactive Discussion](#)



Table 1. Multivariate analyses results. λ_1/λ_2 : individual CCA. Preliminary model coefficients from MAT and WA-PLS2. R_{boot}^2 : bootstrapped coefficient of determination between the observed and predicted values. RMSEP: root mean square error of prediction.

Variable	λ_1/λ_2	% Explained variance	MAT		WA-PLS	
			Boot_ R^2	RMSEP	Boot_ R^2	RMSEP
Salinity*	1.38	15.47	0.83	0.30	0.75	0.33
Nitrate*	0.65	8.14	0.45	0.32	0.39	0.33
Phosphate*	0.25	4.89	0.36	0.02	0.19	0.02
Silicate*	0.22	8.93	0.56	0.24	0.40	0.26
Oxygen*	0.1	1.46	0.15	0.05	0.05	0.05
Chlorophyll <i>a</i>			0.61	0.05	0.58	0.05
Temperature			0.12	0.52	0.07	0.53
Oxygen Saturation			0.20	1.04	0.18	1.02
Mixed Layer Depth			0.31	0.19	0.25	0.19
CO ₃ ²⁻			0.74	0.02	0.70	0.02
pH			0.70	0.02	0.67	0.02
T_{ALK}			0.70	0.00	0.67	0.004
DIC			0.51	13.31	0.48	13.16

* Variables determined by ordination based on AIC.

Development of coccolithophore-based transfer functions

B. Ausín et al.

Title Page

Abstract

Introduction

Conclusions

References

Tables

Figures



Back

Close

Full Screen / Esc

Printer-friendly Version

Interactive Discussion



Table 2. Model coefficients from final MAT and WA-PLS2 cross-validated by bootstrapping for SSS, after removal of one outlier. R_{boot}^2 : bootstrapped coefficient of determination between the observed and predicted values. Max_Bias_{boot} : bootstrapped maximum bias. RMSEP: root mean square error of prediction (psu).

	MAT	WA-PLS2
R_{boot}^2	0.85	0.80
Max_Bias_{boot}	0.23	0.22
RMSEP	0.29	0.30

Development of coccolithophore-based transfer functions

B. Ausín et al.

Table 3. Timing (given in ka cal. BP) of: freshwater advection events (FA) deduced from SSS decreases in core CEUTA10PC08 (this study); cooling events from core MD 95-2043 (ACYD-AC3, Cacho et al., 2001), and continental aridity periods from core ODP Site 976 (YD-APC5, Combourieu Nebout et al., 2009). All cores from the Alboran Sea.

SSS decreases	Cooling events	Continental aridity periods
FA6 13.07–12.06	ACYD 13.1–12.0	YD 12.8–11.75
FA5 11.95–11.71	AC6 11.9–11.65	APC9 11.75–11.4
FA4 11.36–11.00	AC5 11.21–10.95	APC8 11.0–10.8
FA3 10.09–9.83	AC4 10.34–9.95	APC7 10.5–9.8
FA2 9.57–9.21	–	APC6 9.6–8.9
FA1 8.95–7.72	AC3 9.08–7.56	APC5 8.5–7.9

Title Page

Abstract

Introduction

Conclusions

References

Tables

Figures



Back

Close

Full Screen / Esc

Printer-friendly Version

Interactive Discussion



Development of coccolithophore-based transfer functions

B. Ausín et al.

Title Page

Abstract

Introduction

Conclusions

References

Tables

Figures



Back

Close

Full Screen / Esc

Printer-friendly Version

Interactive Discussion

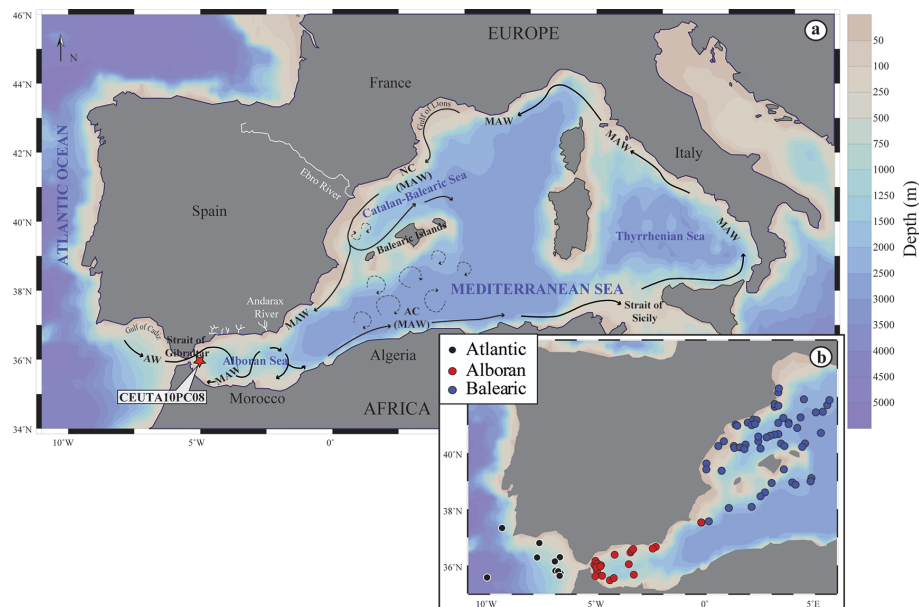


Figure 1. Maps of the study area. **(a)** Location of core CEUTA10PC08 (red star). Black arrows trace general surface circulation. Legend: AW: Atlantic Water. MAW: Modified Atlantic Water. AC: Algerian Current. NC: Northern Current. **(b)** Location of the surface sediment samples in the study area. Maps generated with Ocean Data View software (Schlitzer, 2014).

Development of coccolithophore-based transfer functions

B. Ausín et al.

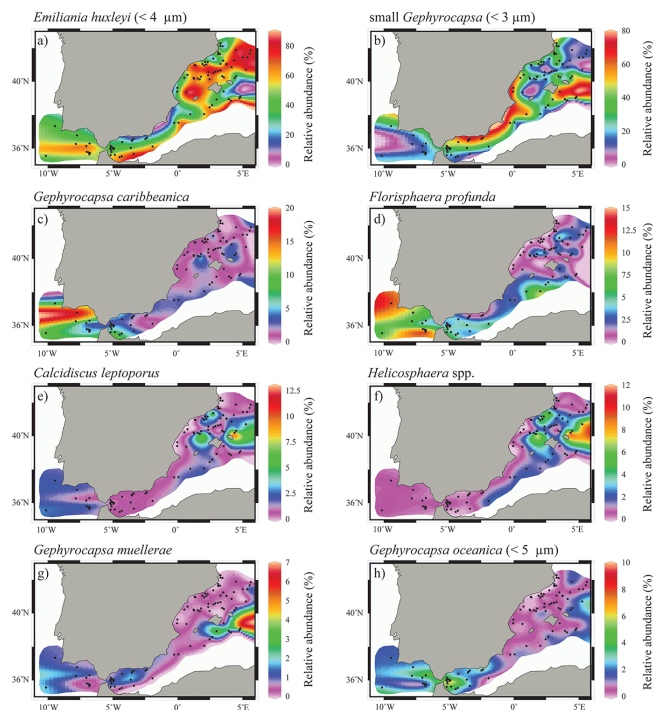


Figure 2. Distribution of the main coccolithophore taxa considered in the training set studied according to their relative abundance (%) in the Western Mediterranean Sea and Atlantic Ocean: **(a)** *Emiliana huxleyi* (< 4 μm). **(b)** small *Gephyrocapsa* (< 3 μm) **(c)** *Gephyrocapsa caribbeanica*. **(d)** *Florisphaera profunda*. **(e)** *Calcidiscus leptoporus*. **(f)** *Helicosphaera* spp. **(g)** *Gephyrocapsa muellerae*. **(h)** *Gephyrocapsa oceanica* (< 5 μm).

[Title Page](#)
[Abstract](#)
[Introduction](#)
[Conclusions](#)
[References](#)
[Tables](#)
[Figures](#)
[Back](#)
[Close](#)
[Full Screen / Esc](#)
[Printer-friendly Version](#)
[Interactive Discussion](#)

Development of coccolithophore-based transfer functions

B. Ausín et al.

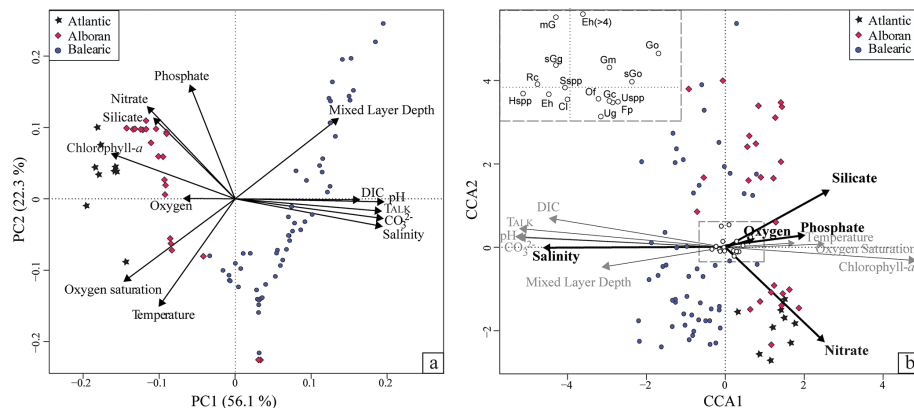


Figure 3. Multivariate analyses. **(a)** PCA based on the initial thirteen environmental variables. **(b)** CCA ordination plot with the site scores scaled by eigenvalues. The 88 sites are represented regarding their location in the Atlantic Ocean, Alboran Sea or Balearic Sea. Active and passive environmental vectors are represented by black and gray arrows, respectively. Scaling for the 16 taxa scores (open circles) is shown on the top left corner. mG: medium *Gephyrocapsa*; Eh (> 4): *Emiliana huxleyi* (> 4 μm); Eh: *Emiliana huxleyi*; sGg: small *Gephyrocapsa*; Gm: *Gephyrocapsa muelleriae*; Go: *Gephyrocapsa oceanica*; sGo: small *Gephyrocapsa oceanica*; Rc: *Rhabdosphaera clavigera*; Sspp: *Syracosphaera* spp.; Of: *Oolithotus fragilis*; Gc: *Gephyrocapsa caribbeanica*; Hspp: *Helicosphaera* spp.; Cl: *Calcidiscus leptoporus*; Usp: *Umbellosphaera* spp.; Ug: *Umbellosphaera* spp.; Fp: *Florisphaera profunda*.

Title Page

Abstract

Introduction

Conclusions

References

Tables

Figures

◀

▶

◀

▶

Back

Close

Full Screen / Esc

Printer-friendly Version

Interactive Discussion



Development of coccolithophore-based transfer functions

B. Ausín et al.

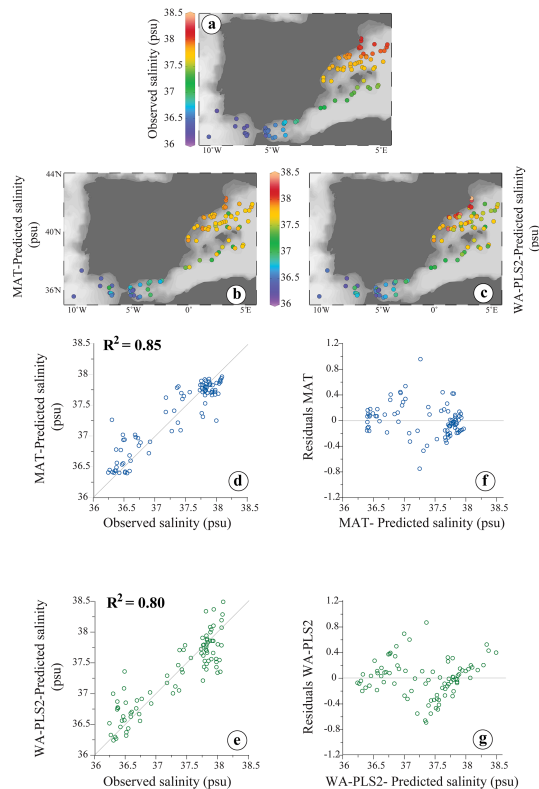


Figure 4. Diagnostic graphs of the models: **(a)** observed salinity values. **(b)** MAT-predicted salinity values. **(c)** WA-PLS2-predicted salinity values. **(d)** Observed vs MAT-predicted salinity values. **(e)** Observed vs WA-PLS2-predicted salinity values. **(f)** MAT-predicted salinity values vs residuals. **(g)** WA-PLS2-predicted salinity values vs residuals.

Title Page

Abstract

Introduction

Conclusions

References

Tables

Figures

◀

▶

◀

▶

Back

Close

Full Screen / Esc

Printer-friendly Version

Interactive Discussion

Development of coccolithophore-based transfer functions

B. Ausín et al.

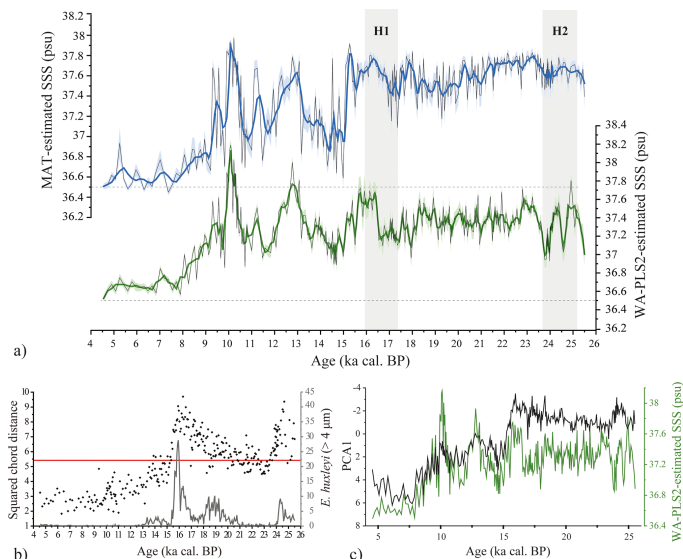


Figure 5. (a) SSS reconstructions for core CEUTA10PC08 derived from MAT (blue) and WA-PLS2 (green). The thin black lines represent the estimated values. The thick blue/green lines represent these original data fitted to a 3-point moving average smoothing spline. Pale blue/green shadows represent the error range, and dashed lines indicate current annual mean SSS in the Alboran Sea from the WOA13 (Zweng et al., 2013). (b) Dissimilarity between modern and fossil assemblages (black dots) measured by squared chord distance (left axis) plotted vs age. The red line indicates the 10th percentile. Relative abundance of the species *E. huxleyi* (> 4 µm) (%; right axis). (c) Profiles comparing the PC1_{fossil} (black line) and WA-PLS2-estimated SSS (green line).

Development of coccolithophore-based transfer functions

B. Ausín et al.

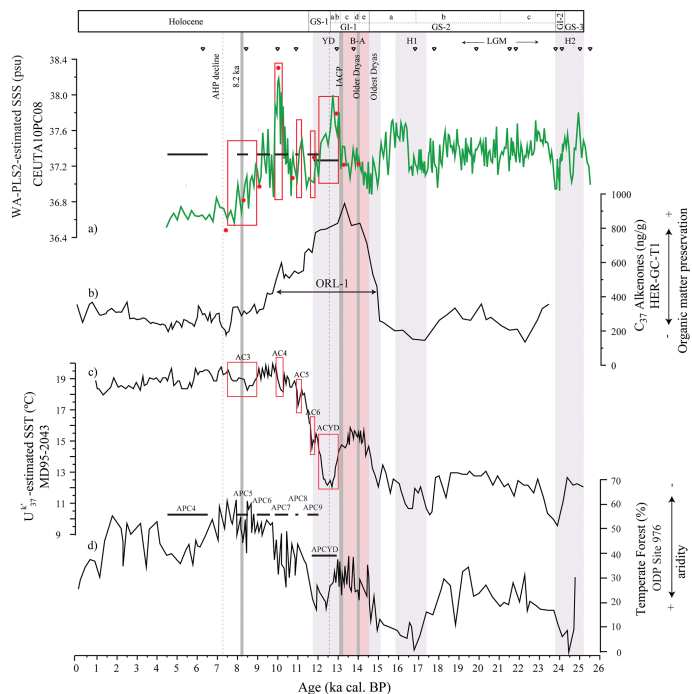


Figure 6. Paleoenvironmental records in the Alboran Sea: **(a)** WA-PLS2-SSS reconstruction (psu) for core CEUTA10PC08. Triangles stand for age control points. **(b)** C₃₇ Alkenones (ng g⁻¹) from core HER-GC-T1 (Ausín et al., 2015). **(c)** SST (°C) from core MD95-2043 (Cacho et al., 2001). Red boxes represent the Alboran cooling events (AC). **(d)** Pollen record (%) from ODP Site 976 (Combourieu Nebout et al., 2009). Horizontal black lines cover the timing of periods of continental aridity (APC).

Title Page

Abstract

Introduction

Conclusions

References

Tables

Figures



Back

Close

Full Screen / Esc

Printer-friendly Version

Interactive Discussion

